Influence of the Crystallization Temperature on the Microphase Morphology of a Semicrystalline ABC Triblock Copolymer

Vittoria Balsamo*,† and Reimund Stadler‡

Grupo de Polímeros USB, Universidad Simón Bolívar, Departamento de Ciencia de los Materiales, Aptdo. 89000, Caracas 1080-A, Venezuela, and Makromolekulare Chemie II, Universität Bayreuth, 95440 Bayreuth, Germany

Received June 25, 1998

ABSTRACT: The microphase morphology of a polystyrene-*block*-polybutadiene-*block*-poly(ϵ-caprolactone) SBC triblock copolymer is studied through transmission electron microscopy. Even though crystallization of the PCL block takes place well below the PS glass transition, lamellar microphases and the formation of well-defined spherulites are observed. The typical long-range order normally obtained for amorphous triblock copolymers is not obtained in the SBC triblock copolymer. The morphology of a polystyrene-*block*-poly(ϵ-caprolactone) diblock copolymer was also observed and compared with the triblock copolymer. To investigate whether the crystallization temperature (T_c) is a parameter influencing the final morphology, samples of the triblock copolymer were crystallized at 45 and 42 °C. This reduction in T_c results in a morphological transition from a simple lamellar morphology (PS, PB, and PCL form layers), which we call lamellar−lamellar (*ll*), to a lamellar−cylindrical (*lc*)-morphology with PS and PCL layers and PB cylinders at the PS/PCL boundary. From these changes, combined with the observation of well-defined spherulites in both cases, we can deduce the orientation of the PCL chains in the crystalline regions as being perpendicular with regard to the block copolymer interfaces.

Introduction

In semicrystalline block copolymers the microphase morphology is influenced by a strong coupling of crystallization and microphase separation. If crystallization proceeds from a homogeneous melt or from a weakly segregated melt in an AB diblock copolymer, it is generally observed that the crystallization process determines the final microphase morphology.[1−5] In this case, a lamellar microphase morphology can be expected, in which the chain axis of the semicrystalline stems are oriented perpendicular to the microdomain interfaces. In contrast, when crystallization takes place from a heterogeneous microphase separated melt, the crystallizable component is "confined" in the preexistent morphology, and chain stems can show a parallel orientation to the interfaces.[6−8] Nevertheless, the actual situation in semicrystalline block copolymers is more complicated, since the segregation level between the components and the glass transition temperature (T_g) of the amorphous block connected to the crystallizable block can influence the way in which the chains in the semicrystalline lamella are oriented. Nojima et al.[9,10] reported that in low molecular weight poly(ϵ-caprolactone)-*b*-polybutadiene diblock copolymers the melt microphase structure is disrupted during subsequent crystallization. This was explained by the fact that the energy to disrupt the rubbery microphase morphology is low as compared to the change in free energy associated with the subsequent crystallization. Similar results were found by Ryan et al.[11] for polyethylene-*b*-polyethylethylene (PE-*b*-PEE) diblock copolymers, due to a moderate degree of melt segregation. On the other hand, Hamley et al.[7,12] found that when poly(vinylcyclohexane) (PVCH) (T_g = 140 °C) is the amorphous but glassy block in a PVCH-*b*-PE diblock copolymer, the morphology is frozen upon cooling below $T_{g(PVCH)}$, and the crystalline chain stems show a parallel orientation with regard to the microdomain interfaces (see Scheme 1).

Scheme 1. (a) Perpendicular and (b) Parallel Orientation of the Crystalline Chain Stems with Respect to the Microdomain Interfaces

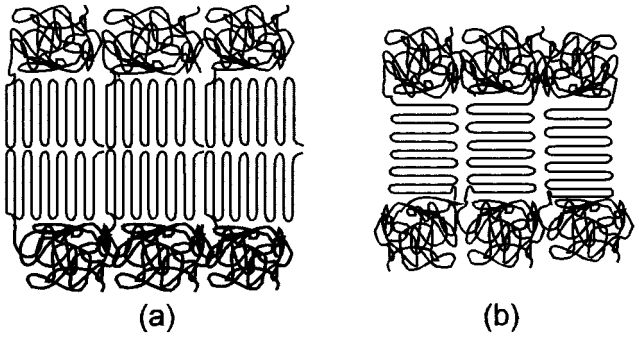

The knowledge about the crystal orientation relative to the microphase boundaries is of key importance to understanding the ultimate mechanical properties of such semicrystalline block copolymers. The situation becomes even more complicated if ternary block copolymers are considered. In previous works we investigated the interplay between crystallization and microphase separation in polystyrene-*b*-polybutadiene-*b*-poly(ϵ-caprolactone) SBC triblock copolymers.[13−16] These copolymers exhibit microphase separation in the melt at the molecular weights considered, with subsequent vitrification of the PS block (around 90−100 °C) and crystallization of the PCL block on cooling.[13,14] Crystallization occurs well below the PS vitrification in a temperature range between 14 and 50 °C, depending on time scale. The variation of the equilibrium melting point of the PCL block with composition, and the formation of spherulites in a broad composition range ($0.48 < \phi_{PCL} < 1.0$), despite the glassy PS block, led us to suggest an

* Corresponding author.
† Universidad Simón Bolívar.
‡ Universität Bayreuth.

10.1021/ma9809942 CCC: $18.00
Published on Web 05/27/1999

orientation of the crystalline chain stems perpendicular to the lamellar microdomains interfaces. In addition, a considerable deformation of the microphase morphology has been observed due to the presence of crystals in the system.[15,16] A striking example is the formation of polygonal core−shell cylinders with PCL core and PB shell in a PS matrix.[16] The situation becomes even more complex in the corresponding hydrogenated block copolymers. Upon hydrogenation of the polybutadiene block with predominant 1,4-microstructure, we obtained polystyrene-*block*-polyethylene-*block*-poly(ϵ-caprolactone) (SEC) triblock copolymers with two crystallizable blocks (linear low-density polyethylene and polycaprolactone).[17,18] Detailed thermal analysis showed that both the PE and the PCL block crystallize. Semicrystalline lamellae of both components coexist. Again the copolymers with more than 50 wt % PCL showed well-defined spherulites formed by the PCL superstructure.

Although several authors have studied the morphology of semicrystalline diblock copolymers, few authors have analyzed the influence of the crystallization conditions or thermal history on the final morphology. The effect of the casting conditions using selective and nonselective solvents and varying the casting temperature have been studied.[1,19,20] Rangarajan et al.[21] found for polyethylene-*b*-head-to-head-polypropylene diblock copolymers a path-dependent microphase morphology. This was attributed to a weak melt segregation, and the formation of spherulites led to support an orientation of the chains in the crystals perpendicular to the microdomain interfaces. Khanpur et al.[22] demonstrated that the melt microphase morphology of a polyethylene-*b*-poly(ethylene-*co*-propylene) diblock copolymer could only be preserved if the sample was quenched in liquid nitrogen. Quiram et al.[5] investigated a series of polyethylene-*b*-poly(3-methyl-1-butene) diblock copolymers of constant composition ($\phi_E = 0.26$). By changing the molecular weight, they were able to cover homogeneous as well as heterogeneous melts in a material in which the glass transition of both blocks is below room temperature. Crystallization in the strongly segregated melts is confined to cylindrical microdomains and produces a morphology that is independent of thermal history. In this case, the chains in the crystals within the cylindrical microdomains are preferentially oriented with the chain axis tilted 18 ± 4° from the normal to the cylinder. This agrees with our previous results in a SBC triblock copolymer with 57 wt % PS, 27 wt % PB, and 16 wt % PCL.[14,18] In contrast, if crystallization takes place from weakly segregated melts, the morphologies found by Quiram et al.[5] are highly dependent on thermal history. Fast cooling confines crystallization to the interior of the cylinders, while slow cooling results in complete disruption of the cylindrical melt mesophases.[5]

In the present contribution we study the influence of the crystallization temperature on the microphase morphology of a SBC triblock copolymer. It will be shown that the manipulation of the microphase morphology helps to get additional information about the orientation of the crystalline chain stems within the microdomains. As a special feature, our SBC triblock copolymers consist of one glassy and one rubbery component at the crystallization temperature of the PCL block.

Experimental Section

Materials. The polystyrene-*block*-polybutadiene-*block*-poly(ϵ-caprolactone) (SBC) triblock copolymer used in the present study was synthesized by sequential anionic polymerization in benzene using *sec*-butyllithium as initiator and diphenylethylene as capping agent for the crossover reaction from polybutadienyl anions to ϵ-caprolactone. Details are described elsewhere.[23] The block copolymer has a number-average molecular weight of 219 000 g/mol and a polydispersity M_w/M_n of 1.30. The number-average molecular weight of the total block copolymer has been determined from the molecular weight of the PS precursor block (calibrated size exclusion chromatography) and the composition determined by ^{1}H NMR spectroscopy. It will be termed as $S_{27}B_{15}C_{58}^{219}$, where the subscripts correspond to the weight percents of the components whereas the superscript equals the total molecular weight in kg/mol. The polybutadiene (PB) block has approximately 90 wt % of 1,4 PB units. A diblock copolymer $S_{37}C_{63}^{80}$ with a polydispersity of 1.18 was also used as a reference material. On the basis of differential scanning calorimetry (DSC) and dynamic mechanical analysis (DMA), $S_{27}B_{15}C_{58}^{219}$ as well as $S_{37}C_{63}^{80}$ is microphase separated and semicrystalline with the following characteristic temperatures:[13]

$S_{27}B_{15}C_{58}^{219}$. DSC (dynamic crystallization at a cooling rate of −20 K/min and various heating rates with extrapolation to heating rate zero): $T_{g(PB)} = -104$ °C; $T_{g(PCL)} = -67$ °C; $T_{m(PCL)} = 54$ °C; $T_{g(PS)} = 95$ °C.

DMA (temperature step mode, 10 rad/s, T_g data taken from the tan δ maximum, T_m data taken as the temperature at $0.5\Delta E'$, with $\Delta E'$ being the drop of the storage modulus associated with melting): $T_{g(PB)} = -88$ °C; $T_{g(PCL)} = -52.5$ °C; $T_{m(PCL)} = 54$ °C; $T_{g(PS)} = 107$ °C.

$S_{37}C_{63}^{80}$. DSC: $T_{g(PCL)} = -70$ °C; $T_{m(PCL)} = 53$ °C; $T_{g(PS)} = 85$ °C.

DMA: $T_{m(PCL)} = 54$ °C; $T_{g(PS)} = 105$ °C.

Transmission Electron Microscopy (TEM). Films (thickness 1 mm) of the triblock copolymer were slowly cast from 5 wt % toluene solutions. For further equilibration the dry films were annealed at 140 °C for 2 h under nitrogen atmosphere. Longer annealing times (up to 5 h) did not affect the morphology. The samples were then cooled to a selected crystallization temperature T_c where they were kept for ∼3 h. Finally, they were quenched to 25 °C.

Ultrathin sections (∼40 nm thick) for transmission electron microscopy were obtained at −120 °C using a FC4 Reichert Ultramicrotome equipped with a diamond knife. The ultrathin sections were stained using osmium tetroxide under vacuum at room temperature. Transmission electron microscopy was performed in the bright field mode on a Phillips transmission microscope, operating at 80 kV.

Results and Discussion

Figure 1 shows a transmission electron micrograph of $S_{27}B_{15}C_{58}^{219}$ crystallized at $T_c = 45$ °C. Due to the staining power of OsO_4, the PB block appears black, the PS block gray, and the PCL block bright. From the micrograph a "simple" lamellar (*ll*)-morphology obeying the layer sequence ···S|B|C C|B|S··· can be assigned to this block copolymer.

Despite the unambiguous assignment of the morphology, the SBC triblock copolymer shows distinct qualitative differences in comparison to totally amorphous triblock copolymers with (*ll*)-morphology: The microdomains do not show the same degree of long-range order as in slowly solution cast amorphous copolymers. In addition, the patterns show in the micrograph some characteristic fold structures. Crystallization obviously has a tremendous influence on the mesophase structure. The fact that this material shows the formation of large spherulites is just another manifestation of this fact.

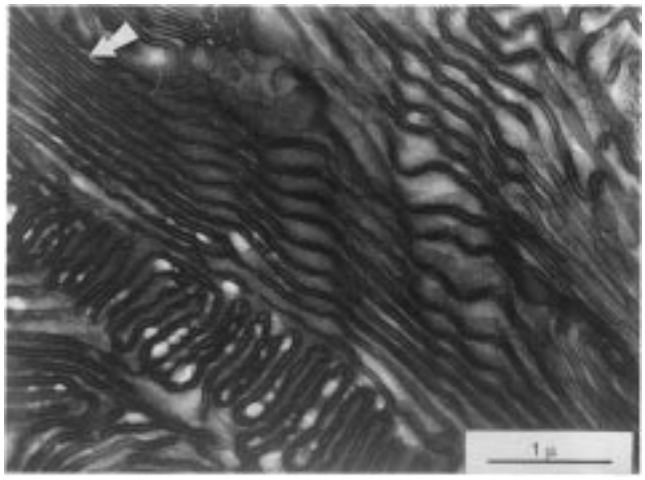

Figure 1. Transmission electron micrograph of $S_{27}B_{15}C_{58}{}^{219}$ crystallized isothermally at 45 °C (stained with OsO_4).

Table 1. Dimensions of the Lamellar−Lamellar (*ll*)-Morphology of $S_{27}B_{15}C_{58}{}^{219}$

dimension	L_{ll}/nm	L_{PS}/nm	L_{PB}/nm	L_{PCL}/nm
measured	109.4 ± 7.1	29.2 ± 6.3	19.4 ± 2.9	41.4 ± 5.4
calcd from vol fractions[a]		25.9	16.7	

[a] To obtain the volume fractions of the components ($\phi_S = 0.275$, $\phi_B = 0.180$, $\phi_C = 0.545$), volume additivity is assumed using the following values of density:[24,25] $\rho_{PS} = 1.05$ g/cm^3; $\rho_{PB} = 0.89$ g/cm^3, and for ρ_{PCL} the expression $(1/\rho_{PCL}) = \tau(1/\rho_{PCL(c)}) + (1 - \tau)(1/\rho_{PCL(a)})$ was applied, where $\rho_{PCL(c)}$ and $\rho_{PCL(a)}$ are the densities of the 100% crystalline PCL (1.20 g/cm^3) and amorphous PCL (1.08 g/cm^3), respectively, and τ is the degree of crystallinity obtained from DSC ($\tau = 0.52$ for $S_{27}B_{15}C_{58}{}^{219}$).

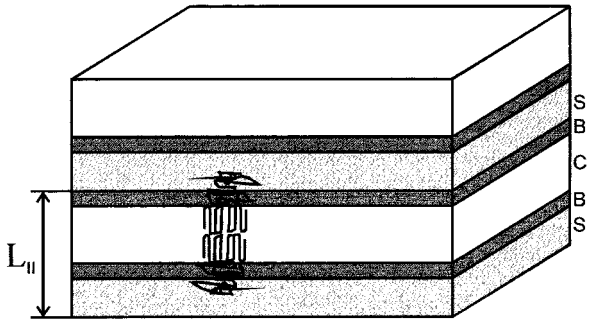

Figure 2. Schematic description of the lamellar−lamellar (*ll*)-morphology.

The PS and PB microdomains have to arrange on a larger scale within the spherulitic superstructure formed by PCL.[13]

Depending on the microtoming direction relative to the orientation of different lamellar stacks, variable thicknesses can be obtained from the TEM. This also holds for amorphous block copolymers. To obtain the "real" long period, the smallest dimensions are most appropriate (see arrow in Figure 1). The dimensions of the microdomains are summarized in Table 1. Figure 2 represents a schematic description of the lamellar−lamellar (*ll*)-morphology. The crystallite orientation within the PCL layer will be discussed below.

From the measured long period L_{ll}, which is the distance obtained from TEM with the highest accuracy, and the volume fractions (ϕ_S, ϕ_B) of the amorphous components, the individual dimensions L_{PS} and L_{PB} were calculated (see Table 1). The calculated dimensions are in good agreement with the values obtained from

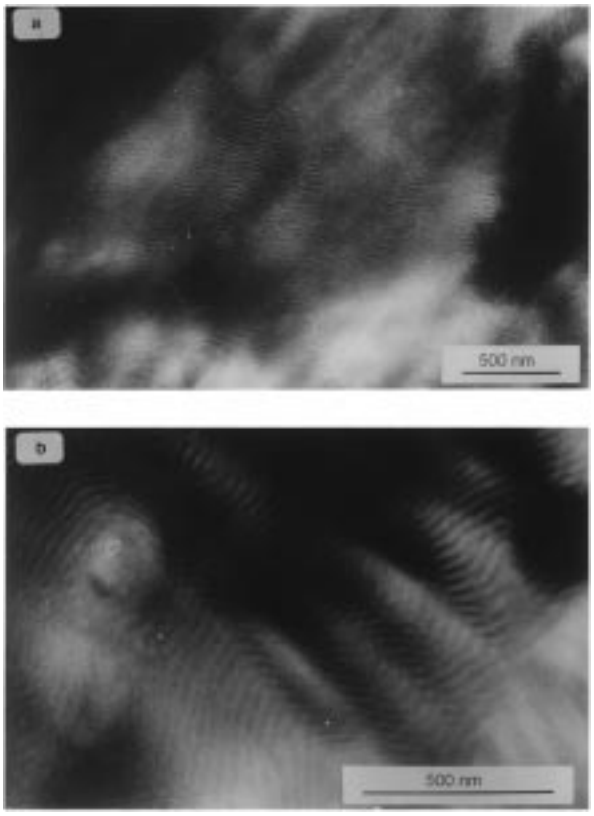

Figure 3. Transmission electron micrograph of $S_{37}C_{63}{}^{80}$ crystallized isothermally at 42 °C (stained with RuO_4).

TEM. Because the PS block is glassy at the PCL crystallization temperature ($\Delta T = T_{g(PS)} - T_{c(PCL)} \approx 55$ deg), the assumption that the dimensions of the PS domains remain unaltered during PCL crystallization seems reasonable. In addition, we estimated the dimensions of the PS domains based on the well-established relation of microdomain dimensions in the strong segregation limit:

$$L \sim N^{2/3}\chi^{1/6} \qquad (1)$$

In a polystyrene-*b*-polybutadiene-*b*-poly(methyl methacrylate) triblock copolymer with a PS block molecular weight of 57K, which is about the same as in the present triblock, the thickness of the PS lamellae was determined to be about 23 nm.[26] Taking this value, the thickness of the PS lamellae in $S_{27}B_{15}C_{58}{}^{219}$ can be estimated using eq 1 to be 24 nm. Within experimental error, this value agrees well with the dimensions determined by TEM.

The lamellar structure of $S_{27}B_{15}C_{58}{}^{219}$ can be compared to a binary SC diblock. For this purpose we have used $S_{37}C_{63}{}^{80}$ with a similar PCL content. On the basis of the composition, a lamellar microdomain morphology might be expected.[27,28] Figure 3 shows transmission electron micrographs of this material in which the PS phase is stained with RuO_4. As expected, a lamellar morphology is obtained. However, some differences can be recognized in comparison with $S_{27}B_{15}C_{58}{}^{219}$. On one hand, the contrast is rather poor in $S_{37}C_{63}{}^{80}$, a result which can be attributed to the partial miscibility of the two blocks. This is supported experimentally by DSC experiments which show a considerable reduction of the PS glass transition temperature (see experimental part).[13] On the basis of an estimation of χ from the Scott−Hildebrandt solubility parameters, this diblock

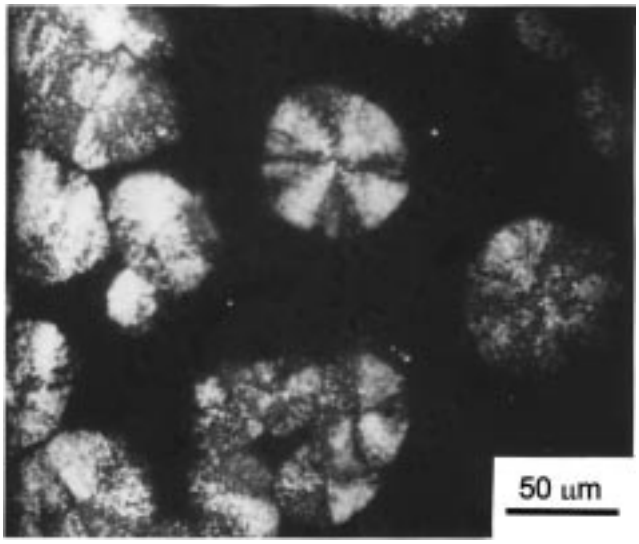

Figure 4. Polarizing optical micrograph of $S_{37}C_{63}^{80}$ isothermally crystallized at 45 °C.

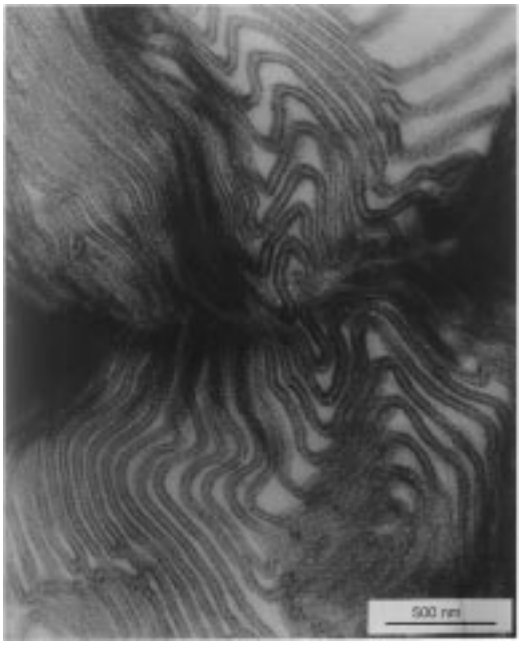

Figure 5. Transmission electron micrograph of $S_{27}B_{15}C_{58}^{219}$ isothermally crystallized at 42 °C (stained with OsO_4).

copolymer is predicted to be in the weak segregation regime ($\chi N = 8.6$). In this block copolymer the system might be miscible in the melt (at the crystallization temperature a homogeneously mixed copolymer would be above the hypothetical glass transition calculated according to the Fox equation), and upon crystallization phase separation occurs into a pure amorphous PCL phase ($T_{g(PCL)} = -70$ °C), a crystalline PCL phase ($T_{m(PCL)} = 53$ °C), and a PS rich glassy mixed phase ($T_{g("PS")} = 85$ °C). This agrees with the observation of distorted spherulites in this diblock copolymer (Figure 4). The presented optical micrograph was obtained from thin films that were cast onto glass slides at room temperature. After allowing the solvent to evaporate slowly, the films were molten at 140 °C and then cooled to the selected crystallization temperature. From the TEM micrographs a long period of 26.0 ± 1.8 nm is obtained. This is considerably smaller than expected for a block copolymer in the strong segregation limit and gives further evidence for the considerable miscibility in the amorphous material. Further studies of this system in which crystallization, phase separation, and vitrification are strongly coupled are needed to get a more comprehensive picture for the diblock copolymers.

Before discussing the influence of the crystallization conditions in the case of $S_{27}B_{15}C_{58}^{219}$, we first compare the observed (*ll*)-morphology in this semicrystalline triblock copolymer to the mesophase structures observed in completely amorphous triblock copolymers of the same composition and a similar balance of the Flory−Huggins interaction parameters $\chi_{BC} > \chi_{AB} \gg \chi_{AC}$. This is realized in polystyrene-*block*-polybutadiene-*block*-poly(methyl methacrylate) (SBM) triblock copolymers.[29,30] SBM triblock copolymers of similar composition ($\phi_B/\phi_A = 0.650$; $\phi_A + \phi_B = 0.455$) are close to the borderline between lamellar and cylindrical morphological families.[33] In the case of a cylindrical morphology one would expect a c_ac morphology (for description see refs 30 and 33). However, on the basis of the PCL volume fraction, a lamellar morphology should be slightly preferred. For a lamellar morphology one would expect either a (*ll*)- or a (*lc*)-morphology because of the small PB volume fraction $\phi_B = 0.17$ and the thermodynamic balance of the three binary interaction parameters,[29] with a preference for the (*lc*)-morphology. These predictions are based on the simple extension of the Semenov−Alexander−de Gennes model to ternary block copolymers.[29,30] The calculations assumed constant segmental volumes and identical segment length. Variations in these quantities will alter the phase boundaries to some extent. However, these calculations do not take into account the influence of crystallization.

As mentioned in the Introduction, there are few reports studying the influence of crystallization conditions on the microphase morphology. Moreover, studies have been limited to investigate the effect of the cooling rate.[5,21,22] One of the parameters that might have a pronounced influence on the microphase morphology, and that to our knowledge had not been studied before, is the crystallization temperature. Crystallization at various temperatures will lead to the formation of crystalline lamella of different thickness. This should influence the stretching of all other components and might influence the microphase morphology.

In addition to the isothermal crystallization at 45 °C, which resulted in the (*ll*)-morphology, $S_{27}B_{15}C_{58}^{219}$ was crystallized isothermally at 42 °C. Figure 5 shows a TEM micrograph of this sample. It is immediately obvious that the morphology has changed as compared to Figure 1. The overall morphology is still lamellar; however, the OsO_4 stained polybutadiene microphases do not form anymore a continuous layer. Separated PB microdomains can be distinguished at the PS|PCL interface. Since these microdomains are regularly ordered at the phase boundary between the two lamellae, they can be assigned as PB cylinders. We thus can assign a lamellar−cylindrical (*lc*)-morphology as schematically shown in Figure 6 to $S_{27}B_{15}C_{58}^{219}$, which was crystallized at 42 °C. The dimensions for the different microphases are summarized in Table 2. The overall lamellar long period L_{lc} is approximately 61 nm. From the composition, the diameter of the cylinders D_{PB} could be calculated according to eq 2 to be 14.4 nm, which is in agreement with the dimensions taken from the

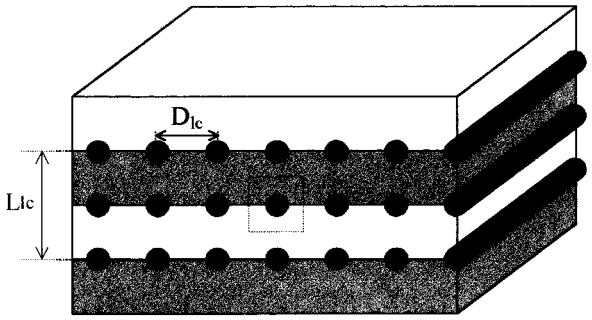

Figure 6. Schematic description of the lamellar−cylindrical (*lc*)-morphology.

Table 2. Dimensions of the Lamellar−Cylindrical (*lc*)-Morphology of $S_{27}B_{15}C_{58}$[219]

dimension	L_{lc}/nm	L_{PS}/nm	L_{PCL}/nm	D_{PB}/nm	D_{lc}/nm
measured	60.5 ± 1.6	31.7 ± 1.6	31.7 ± 2.7	12.8 ± 1.5	28.9 ± 3.2
calculated				14.4[a]	

[a] Diameter of the PB cylinders, calculated according to eq 2.

micrographs (12.8 nm).

$$D_{PB} = 2\sqrt{\frac{\phi_{PB}(L_{lc}/2)^2}{\pi}} \qquad (2)$$

The calculation was made using the unit cell depicted in Figure 6. This calculation is based on the assumption that the distance between the cylinders D_{lc} is about half the overall long period. In other words, it is assumed that the stretching of the end blocks parallel and perpendicular to the A|C interface is the same. This is supported by the experiment which shows that L_{PS} is about the same as D_{lc} (see Table 2).

Comparison of the microdomain dimensions of $S_{27}B_{15}C_{58}$[219] crystallized at 42 and 45 °C shows some pronounced differences: The overall long period is strongly reduced at $T_c = 42$ °C (60.5 nm in comparison to 109.4 nm). A reduction of the long period by about 20−25% when switching from the (*ll*)- to (*lc*)-morphology is expected theoretically[29] and has been observed experimentally by small-angle X-ray scattering.[31] However the variation of the long period at the different crystallization temperatures is considerably larger. Most striking is the large difference in the thickness of the PCL layer. The PCL microdomains crystallized at $T_c = 45$ °C have a thickness of about 41 nm, while at $T_c = 42$ °C the PCL layer thickness is only about 32 nm. It can be expected that crystallization at lower temperature leads the formation of thinner crystals. This will be reflected in the thickness of the PCL layer if the number of semicrystalline layers in the PCL microdomains is the same. Under this assumption, the TEM results, together with the observation of well-defined spherulitic superstructures in both cases, give strong evidence toward a perpendicular orientation of the crystalline chain stems with respect to the lamellar direction. In a previous work on solution grown crystals of a $S_{35}B_{15}C_{50}$ triblock copolymer such orientation was already discussed.[32] In our case ($S_{27}B_{15}C_{58}$) a reduction of the PCL microdomain size upon lowering T_c indicates an increase of the fold number and therefore a larger crystal surface. To accommodate such a larger crystal surface, the overall long period has to become smaller. If a (*ll*)-morphology would be retained, the surface free energy would increase considerably because of the highly unfavorable interaction between the PB center block and the end blocks. On the other hand, the *(lc)*-morphology avoids a thermodynamically unfavorable stretching of the PB block. Therefore, the morphological transition from a *(ll)*-morphology to a *(lc)*-morphology upon reduction of the crystallization temperature can be qualitatively explained as the "rupture" of the PB lamellae to form PB cylinders upon decreasing the crystal thickness. This is schematically shown in Figure 7. The resulting new PS/PCL interface is less unfavored than PB/PCL interfaces. One of the key issues that remains open at the moment and is going to be investigated in the future relates to the number of crystalline lamellae within the PCL layer.

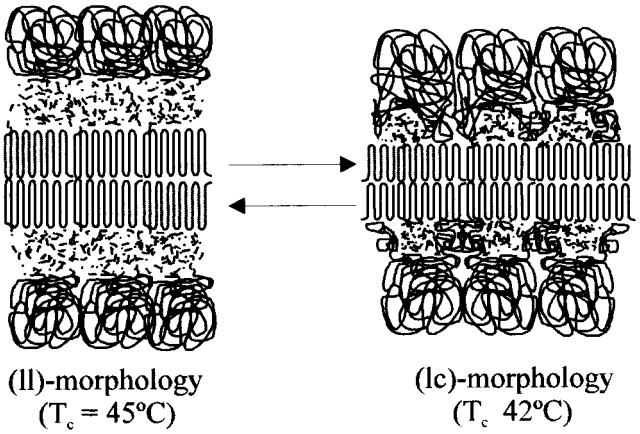

Figure 7. Schematic description of the morphological transition from a (*ll*)- to a (*lc*)-morphology upon reducing the crystallization temperature from 45 to 42 °C.

Conclusions

The study of the microphase morphology of $S_{27}B_{15}C_{58}$ through transmission electron microscopy showed that the presence of a crystallizable block in an ABC triblock copolymer has a tremendous influence on the mesophase structure. The microdomains do not show the same degree of long-range order as in amorphous ABC triblock copolymers. Moreover, a change of the crystallization conditions can induce a morphological transition.

We demonstrated that a lowering of the crystallization temperature induces a morphological transition from a lamellar−lamellar *(ll)*- to a lamellar−cylindrical *(lc)*-morphology due to the rupture of the PB lamellae to form PB cylinders. This occurs in order to avoid a thermodynamically unfavorable stretching of the PB block and to avoid the increase of surface free energy that would take place due to the unfavorable interaction between the PB center block and the end blocks. These results together with the previously demonstrated formation of well-defined spherulites give strong evidence of a perpendicular orientation of the crystalline PCL chain stems with regard to the block copolymer interfaces.

Acknowledgment. This work was supported by BMBF and BASF through joint grant 03M40861. V.B. acknowledges the support of the CONICIT through project S1-96001934 and of the "Decanato de Investigación y Desarrollo" of the USB through grant GID-DID-G02. The authors are indebted to A. Müller (USB) and V. Abetz (UBT) for numerous discussions.

References and Notes

(1) Hirata, E.; Ijitsu, T.; Soen, T.; Hashimoto, T.; Kawai, H. *Polymer* **1975**, *16*, 249.
(2) Rangarajan, P.; Register, R. A.; Fetters L. J. *Macromolecules* **1993**, *26*, 4649.
(3) Rangarajan, P.; Register, R. A.; Adamson, D. H.; Fetters, L. J.; Bras, W.; Naylor, S.; Ryan, A. J. *Macromolecules* **1995**, *28*, 1422.
(4) Yang, Y. W.; Tanodekaew, S.; Mai, S. M.; Boothe, C.; Ryan, A. J.; Bras, W.; Viras, K. *Macromolecules* **1995**, *28*, 6029.
(5) Quiram, D. J.; Register, R. A.; Marchand, G. R. *Macromolecules* **1997**, *30*, 4551.
(6) Cohen, R. E.; Bellare, L.; Drzewinski, M. A. *Macromolecules* **1994**, *27*, 2321.
(7) Hamley, I. W.; Fairclough, J. P. A.; Terrill, N. J.; Ryan, A. J.; Lipic, P. M.; Bates, F. S.; Towns-Andrews, E. *Macromolecules* **1996**, *29*, 8835.
(8) Unger, R.; Beyer, D.; Donth, E. *Polymer* **1991**, *32*, 3305.
(9) Nojima, S.; Kato, K.; Yamamoto, S.; Ashida, T. *Macromolecules* **1992**, *25*, 2237.
(10) Nojima, S.; Nakano, H.; Takahashi, Y.; Ashida, T. *Polymer* **1994**, *35*, 3479.
(11) Ryan, A. J.; Hamley, I. W.; Bras, W.; Bates, F. S. *Macromolecules* **1995**, *28*, 3860.
(12) Hamley, I.; Fairclough, J. P. A.; Ryan, A. J.; Bates, F. S.; Towns-Andrews, E. *Macromolecules* **1996**, *29*, 4425.
(13) Balsamo, V.; von Gyldenfeldt, F.; Stadler, R. *Macromol. Chem. Phys.* **1996**, *197*, 3317.
(14) Balsamo, V. PhD Thesis, University of Mainz, 1996.
(15) Balsamo, V.; Stadler, R. *Macromol. Symp.* **1997**, *117*, 153.
(16) Balsamo, V.; von Gyldenfeldt, F.; Stadler, R. *Macromolecules*, submitted for publication.
(17) Balsamo, V.; Müller, A. J.; von Gyldenfeldt, F.; Stadler, R. *Macromol. Chem. Phys.* **1998**, *199*, 1063.
(18) Balsamo, V.; Müller, A. J.; Stadler, R. *Macromolecules* **1998**, *31*, 7756.
(19) Seguela, R.; Prud'homme, J. *Polymer* **1989**, *30*, 1446.
(20) Cohen, R. E.; Cheng, P. L.; Douzinas, K.; Kofinas, P.; Berney, C. V. *Macromolecules* **1990**, *23*, 324.
(21) Rangarajan, P.; Register, R. A.; Fetters, L. J.; Bras, W.; Naylor, S.; Ryan, A. J. *Macromolecules* **1995**, *25*, 4932.
(22) Khandpur, A. K.; Macosko, C. W.; Bates, F. S. *J. Polym. Sci., Part B: Polym. Phys.* **1995**, *33*, 247.
(23) Balsamo, V.; von Gyldenfeldt, F.; Stadler, R. *Macromol. Chem. Phys.* **1996**, *197*, 1159.
(24) Herman, J. J.; Jerome, R.; Teyssiè, P.; Gervais, M.; Gallot, B. *Makromol. Chem.* **1981**, *182*, 997.
(25) *Polymer Handbook*, 3rd ed.; Brandrup, J., Immergut, E. H., Eds.; J. Wiley & Sons: New York, 1989.
(26) Auschra, C.; Stadler, R. *Macromolecules* **1993**, *26*, 2171.
(27) Whitmore, M. D.; Noolandi, J. *Macromolecules* **1988**, *21*, 1482.
(28) DiMarzio, E. A.; Guttman, C. M.; Hoffman, J. D. *Macromolecules* **1980**, *13*, 1194.
(29) Stadler, R.; Auschra, C.; Beckmann, J.; Krappe, U.; Voigt-Martin, I. G.; Leibler, L. *Macromolecules* **1995**, *28*, 3080.
(30) Breiner, U.; Krappe, U.; Abetz, V.; Stadler, R. *Macromol. Chem. Phys.* **1997**, *198*, 1051.
(31) Breiner, U.; Stadler, R.; Thomas, E. L., to be published. Breiner, U. Ph.D. Thesis, University of Mainz, 1997.
(32) Jackson, C. L.; Chanzy, H. D.; Han, C. C.; Balsamo, V.; Stadler, R. *Abstracts of the American Chemical Society, PMSE* **1997**, *77*, 650.
(33) Examples for lamellar morphologies:[29] *ll (simple lamellar)*: A, B, and C form continuous layers; *lc (lamella with cylinders)*: B forms cylindrical microdomains at the interface between A and C layers; *ls (lamella with spheres)*: B forms spherical (or ellipsoidal) microdomains at the interface between A and C layers; other lamellar morphologies: *cl (cylinders in one layer) and cs (spheres in one layer)*: two components form a lamellar structure, and one minority end block forms cylinders (or spheres) in the layer of the chemically adjacent block. Examples for cylindrical ABC morphologies with one of the end blocks forming the matrix[30] (C will be taken in the following as the matrix forming component for simplicity): c_ic *(cylinder in cylinder)*: core−shell cylinders (A = core, B = shell); c_ac *(cylinders at cylinder)*: A forms cylinders with a certain number of B cylinders with their cylinder axis parallel to the A cylinder on the surface; other examples are described in ref 30.

MA9809942